ELSEVIER

Journal of Photochemistry and Photobiology A: Chemistry 90 (1995) 45–51

Journal of PHOTOCHEMISTRY AND PHOTOBIOLOGY A:CHEMISTRY

Picosecond polarized pump–probe spectroscopy of amylose–iodine

Archita Sengupta, Manickam Neelakandan, Pei-Pei Tang [1], Miin-Liang Horng [2], Edward L. Quitevis *

Department of Chemistry and Biochemistry and Institute for Biotechnology, Texas Tech University, Lubbock, TX 79409, USA

Received 24 November; accepted 16 February 1995

Abstract

Single-wavelength picosecond polarized pump–probe spectroscopy has been used to study the excited state dynamics of aqueous suspensions of the amylose–iodine complex at wavelengths within the broad absorption band centered at about 635 nm. A single-exponential fit of the magic angle signal at 600 nm gave an average ground state recovery time of 870 ± 50 ps. For excitation at 570 nm a bi-exponential decay with a short component of about 160 ps and a long component of 870 ps gave the best fit of the magic angle signal. The non-exponential decay is attributed to overlapping absorption and relaxation processes due to different polyiodide chains. Since no fluorescence is observed from the complex, the pump–probe signals must be due to relaxation from a long-lived excited state which is not part of the singlet manifold of states. No excitation intensity dependence was observed in the decay kinetics. The anisotropy was constant over the time range of our experiment. The value of the anisotropy was about 0.35 ± 0.04, which is less than the maximum theoretical value of the initial anisotropy, $r_0 = 0.4$. These results are shown to be consistent with a five-level model.

Keywords: Picosecond pump–probe spectroscopy; Starch–iodine complex; Polymers; Polyiodides

1. Introduction

Quasi-one-dimensional molecular systems have attracted much attention in recent years because of their potential as novel electronic and optical materials [1]. Linear chains of polyiodide anions are of particular interest [2,3]. When polyiodide anions are incorporated into solvent-free polymer electrolytes [4] and conducting and semiconducting polymers (i.e. polysulfurnitride and polyacetylene) [5,6], the electrical conductivities of the resulting composite materials are higher than those of the polymers themselves. The starch–iodine complex, which has long been used as a colored indicator for both quantitative and qualitative analysis [7], is a well-known example of such polymer–polyiodide composites. Starch is a homopolysaccharide with two polymeric parts: α-amylose and amylopectin. α-Amylose is the linear helical component of starch and consists of long unbranched chains of 1,4-linked α-D(+)-glucopyranose units [8]. Amylose forms an intense blue–black adduct with aqueous iodine in the presence of iodide or with iodine vapor [9]. This complex has a broad absorption band centered at about 635 nm. Although the starch–iodine complex has been studied for many years, information about the structure of the chromophore that gives rise to the blue–black color has been ambiguous [9]. In a series of early potentiometric and spectrophotometric titration studies and optical and X-ray diffraction experiments, Rundle and coworkers [10] found that a complex of definite composition was formed between amylose and iodine. The iodine component of this complex is a unidimensional array within an amylose helix of diameter about 13 Å and period 8 Å with six glucose residues per turn. Because both I_2 and I^- are needed to form the complex, it was widely thought that the repeat unit in the iodine chain was the triiodide ion I_3^- [11]. Marks and coworkers [12] have recently shown, however, that the resonance Raman and iodine-129 Mössbauer spectra of solid starch–iodine are remarkably similar to those of polycrystalline (trimesic acid $\cdot H_2O)_{10} \cdot H^+I_5^-$. The pentaiodide ion in this compound is linear. The bonding in I_5^- and other polyiodides is due to a Lewis acid–base interaction with I_2 acting as the Lewis acid and I^- as the Lewis base. Based on the similarity of the spectra, Marks and coworkers concluded that iodine is complexed to amylose predominantly in the form of I_5^- and not, as previously speculated, in the form of I_3^- and that the color of amylose–iodine must largely be due to optical transitions

* Corresponding author.

[1] Present address: Department of Chemistry, Stanford University, Stanford, CA 94305, USA.

[2] Present address: Department of Chemistry, The Pennsylvania State University, University Park, PA 16802, USA.

SSDI 1010-6030(95)04067-6

in $(I_5^-)_x$ chains. They also suggested that there might be a connection between the I_5^- repeat distance (15.5 Å) and twice the dimension of the pitch of the amylose helix (about 16 Å) [12b].

In this paper we describe the first picosecond polarized pump–probe spectroscopic study of the excited state dynamics of aqueous suspensions of the amylose–iodine complex. Our motivation in studying the amylose–iodine complex stems partly from the fact that the photophysics of this complex is not well known. The amylose–iodine complex is a form of molecular aggregate which exhibits strong interactions between the monomer units. Understanding the excited state dynamics of such strongly interacting systems has been a major focus of research in our laboratory for the past several years [13]. Because amylose–iodine does not fluoresce, standard time-resolved luminescence techniques cannot be used. Information about the excited state processes in the complex can be obtained instead by using transient absorption techniques.

2. Experimental details

Varying concentrations (0.15–0.7 g l^{-1}) of aqueous amylose stock solutions were prepared with potato amylose (Sigma). This type of amylose (type III) is essentially amylopectin free. A weighed amount of amylose was added to a volume of deionized water. The mixture was stirred overnight at a temperature of about 90 °C. Not all of the amylose was dissolved by this method. To determine the actual amylose concentration, the undissolved amylose was removed by filtration. The filter paper containing the undissolved amylose was dried and weighed to determine the amount of amylose that did not dissolve in water. Deionized water was added to the volume of the filtered solution to make up the desired concentration of aqueous amylose. Saturated iodine stock solutions in excess potassium iodide (I_2/KI) of varying concentrations were prepared from resublimed iodine and stored in a cool dark place. Solutions of the amylose–iodine complex were prepared by mixing proportions of the amylose and I_2/KI stock solutions with further dilutions. In the final samples the amylose concentration was varied from 0.02 to 0.08 g l^{-1}, the I_2 concentration was varied from 0.081 to 0.46 mM and the KI concentration was varied from 0.2 to 0.9 mM. In order to prevent bacterial action in the amylose solutions, the amylose–iodine solutions were made freshly prior to the measurement of the absorption spectra and the pump–probe transients. The absorption spectra of the solutions were taken regularly to check for degradation. The absorption spectra of the solutions were recorded in quartz cuvettes of 1 mm path length at room temperature (21 ± 1 °C) on a Shimadzu 265 UV–visible spectrophotometer using aqueous amylose as the reference. Fluorescence measurements were performed on an SLM 4800C spectrofluorometer using front-face illumination.

The picosecond pump–probe apparatus used in this study has been described previously [13]. Two excitation sources were used. The first source was a synchronously pumped double-jet dye laser (rhodamine 6G gain dye, DODCI saturable absorber dye) with a single-plate birefringent filter which gave 2 ps pulse autocorrelation widths at 600 nm. To obtain shorter wavelength excitation, we used a synchronously pumped single-jet dye laser (rhodamine 110) with a three-plate birefringent filter which gave 10 ps pulse autocorrelation widths at 570 nm. The repetition rate for both lasers was about 76 MHz. The dye laser beam was split into non-collinear, co-propagating pump and probe beams with a Michelson interferometer. The beams were focused with an achromat of 10 cm focal length to a spot size of about 200 μm in a rotating cell of 3 mm path length. The average laser powers in the pump and probe beams were 14 and 10 mW respectively. A microcomputer-controlled translation stage in the probe arm of the apparatus was used to delay the time of arrival of the probe pulse with respect to the pump pulse in the sample. The pump beam was modulated at 10.24 MHz with an acousto-optic modulator before being focused into the sample. The modulation induced on the probe beam was detected with a photodiode whose output was amplified and fed into a megahertz lock-in amplifier. The polarization of the probe beam with respect to the pump beam was changed with a polarization rotator. The polarized bleaching signals $S_{\parallel}(t)$ and $S_{\perp}(t)$ and the isotropic bleaching signal $S_{54.7^{\circ}}(t)$ were obtained with probe light polarized parallel, perpendicular and 54.7° (the "magic" angle) to the polarization of the excitation beam respectively. The background-free second-order autocorrelation of the pulse was determined by replacing the sample with a KDP crystal and measuring the second-harmonic generation signal as a function of probe delay. The maximum of the autocorrelation was used to establish the position of zero delay. All measurements were carried out at room temperature.

3. Results

Fig. 1 shows the absorption spectra of the blue–black amylose–iodine solutions containing a fixed amylose concentration of 0.08 g l^{-1} and varying concentrations of I_2/KI. The broad absorption band centered at about 635 nm, which is due to the formation of the amylose–iodine complex, is clearly evident in the spectra. In addition, absorption bands appear at 225 and 196 nm due to free I^- and at 351 and 288 nm due to free I_3^- [14]. With increasing iodine content the broad band (about 200 nm full width at half-maximum (FWHM)) centered at 635 nm grows but eventually reaches saturation, whereas the bands due to free I^- and I_3^- continue to grow. No fluorescence was detected from the sample. Pump–probe experiments were carried out on those samples corresponding to the fully saturated complex and which gave absorbances of about 0.2 in a cell of 1 mm path length.

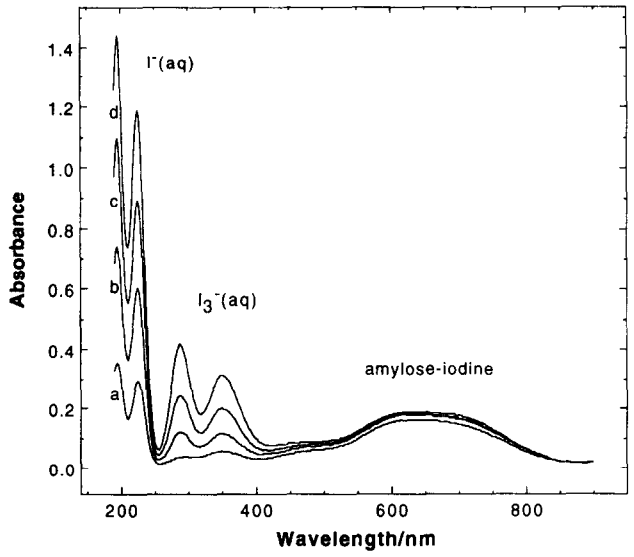

Fig. 1. Absorption spectra of 0.084 g l^{-1} aqueous amylose solutions with varying amounts of I_2/KI: a, 0.081 mM/0.23 mM; b, 0.16 mM/0.45 mM; c, 0.24 mM/0.68 mM; d, 0.32 mM/0.91 mM. The spectra were taken in quartz cuvettes of 1 mm path length using a 0.084 g l^{-1} aqueous amylose solution without iodine as the reference.

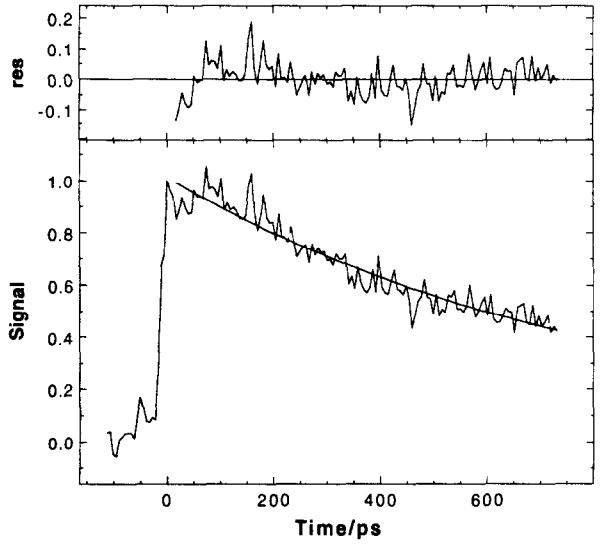

Fig. 2. Normalized magic-angle-induced transmission signal $S_{54.7°}(t)$ for excitation at 600 nm. The full line through the signal is a fit of the data to an exponential decay function with decay time 847 ps ($\chi^2 = 0.35$). Plotted above the signal are the residuals from the fit.

For this absorbance, optimum pump–probe signals were obtained.

Fig. 2 shows a normalized 600 nm magic-angle-induced transmission signal for a fully saturated complex. The sharp peak at zero time is the coherent coupling spike. Because the signal decays on a time scale much longer than the width of pulse autocorrelation, it was not necessary to deconvolute the decay function from the signal. Fits were started at 10 ps instead of at zero delay to avoid the effect of the finite width of the pulse. For excitation at 600 nm a single-exponential decay function best described the time dependence of the signal, as indicated by the random residuals (Fig. 2). Analysis of several data sets yielded an average recovery time of 870 ± 50 ps. Decreasing the excitation intensity by half had no effect on the decay kinetics of the magic angle signals at either of the two wavelengths. Increasing the iodine-to-amylose ratio also had no effect on the decay kinetics, which is consistent with the complex being near saturation. The samples were stable under laser irradiation for extended periods of time, as evidenced by the absorption spectra of the laser-irradiated samples which were identical with absorption spectra of fresh samples. We conclude that the observed signals must be due primarily to photophysical processes and not to any photochemical process that could lead to permanent products.

The absorption anisotropy $r(t)$ is defined by

$$r(t) = \frac{S_{\parallel}(t) - S_{\perp}(t)}{S_{\parallel}(t) + 2S_{\perp}(t)} \quad (1)$$

The anisotropy measures depolarization effects due to the overall rotational motion of the complex, level kinetics and/or transport of the excitation energy along the polyiodide chain. In the time range of our measurements (0–700 ps) the overall rotational motion of the aggregate is not expected to contribute to the decay of the anisotropy. Therefore $r(t)$ will be determined primarily by level kinetics and/or excitation energy transport in the polyiodide chain. Fig. 3(a) shows the parallel and perpendicular induced transmission signals for excitation at 600 nm. The anisotropy calculated from these

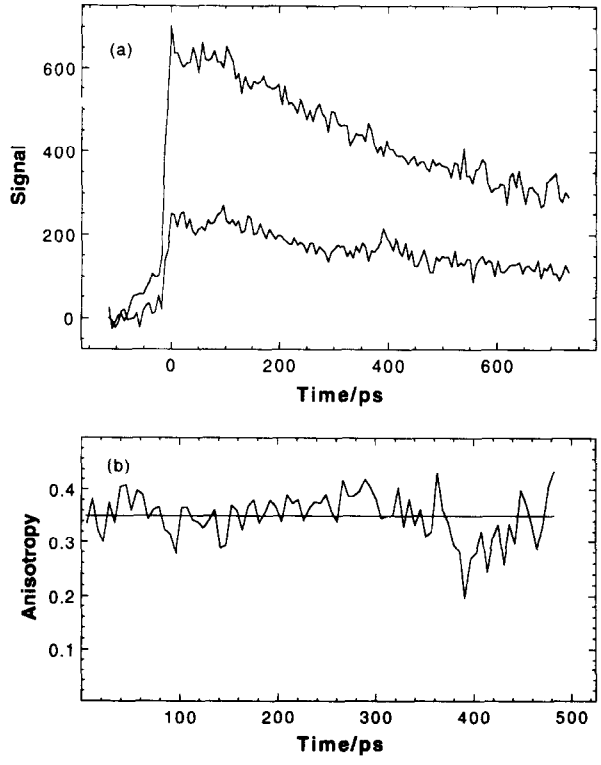

Fig. 3. (a) Induced transmission signal for excitation at 600 nm for probe light polarized parallel to the pump light (upper curve) and probe light polarized perpendicular to the pump light (lower curve). (b) Absorption anisotropy $r(t)$ calculated from Eq. (1) by using the signals in (a). The full line through the anisotropy is the average value of 0.35 ± 0.04.

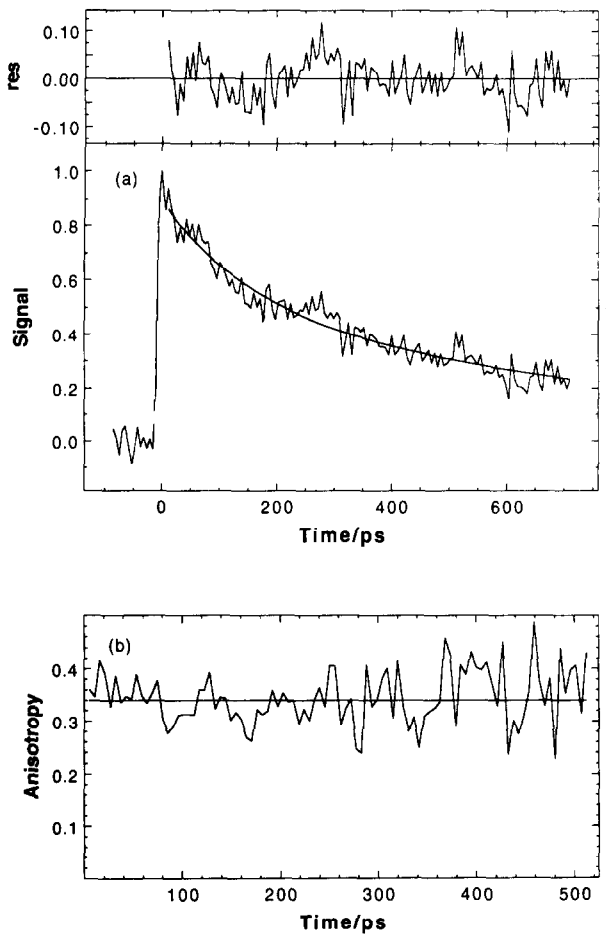

Fig. 4. (a) Normalized magic-angle-induced transmission signal $S_{54.7°}(t)$ for excitation at 570 nm. The full line through the signal is a fit of the data to a bi-exponential decay function $f(t) = 0.37\ \exp(-t/155\ \text{ps}) + 0.52\ \exp(-t/870\ \text{ps})$ ($\chi^2 = 0.254$). Plotted above the signal are the residuals from the fit. (b) Absorption anisotropy $r(t)$ for excitation at 570 nm. The full line through the anisotropy is the average value of 0.34 ± 0.05.

signals (Fig. 3(b)) is constant in the indicated time range and has a value of 0.35 ± 0.04, which is less than the maximum theoretical value of 0.4.

In contrast, the signal at 570 nm is clearly non-exponential (Fig. 4(a)) and can be well described by a bi-exponential decay function, with residuals of the fit being random. In addition to the 870 ps relaxation, a relaxation time of about 160 ps appears for excitation at 570 nm. The anisotropy at 570 nm (Fig. 4(b)) is 0.34 ± 0.05, which within experimental error is the same value as that at 600 nm.

4. Discussion

To explain the pump–probe data, we make use of a five-level model (Fig. 5). This model is an extension of the three-level model used by Alavi et al. [15] to describe the picosecond polarization spectroscopy of dyes in solution. In the three-level model $|0\rangle$, $|1\rangle$ and $|2\rangle$ are states in the singlet manifold. Our model incorporates a second manifold of states. State $|3\rangle$ is a long-lived state which is optically inaccessible (or very weakly forbidden) from the ground state and can only be populated by non-radiative decay from $|1\rangle$. For this reason we will refer to these states as "dark" states. State $|4\rangle$ allows us to account for the possibility of excited state absorption within this second manifold. This second manifold of levels could be associated with triplet states, charge transfer states of the complex or photoproducts that eventually recombine to regenerate the complex within the time scale of the measurement. Given the wavelength limitations of our apparatus, we are unable to identify the nature of these states at this time. None the less, as we will show below, such states must play an important role in the photophysics of the amylose–iodine complex.

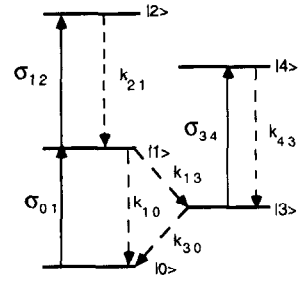

Fig. 5. Five-level model for amylose–iodine complex. The $\{\sigma_{ij}\}$ are absorption cross-sections coupling states $|i\rangle$ and $|j\rangle$; $\{k_{ij}\}$ are first-order constants for relaxation between states $|i\rangle$ and $|j\rangle$.

The amylose–iodine complex interacts with the probe light through the transition dipole moment $\boldsymbol{\mu}^{ij}$ which couples state $|i\rangle$ and state $|j\rangle$ with the cross-section σ_{ij}. Because vibrational relaxation is rapid compared with the time resolution of our apparatus (2–10 ps), vibrational levels are not included in this model. The level kinetics are characterized by first-order constants k_{ij} for decay between states $|i\rangle$ and $|j\rangle$. Furthermore, within the time resolution of our apparatus, transitions from $|2\rangle$ to $|1\rangle$ and from $|4\rangle$ to $|3\rangle$ are so rapid (i.e. $k_{21} \approx \infty$ and $k_{43} \approx \infty$) that the populations in $|2\rangle$ or $|4\rangle$ are essentially zero. This model is not unreasonable and provides a means of analyzing the level kinetics for many molecular systems. Mizuno et al. [16] have shown by using Hückel molecular orbital calculations that the density of excited states in $(I_5^-)_x$ chains is high, which enhances the probability of excited state absorption in these systems.

Solving the set of coupled first-order differential equations for the state populations $K^{(i)}$ yields

$$K^{(4)}(t) \approx 0 \tag{2a}$$

$$K^{(3)}(t) = K^{(1)}(0)\,\frac{k_{13}}{k_1 - k_{30}}\,[\exp(-k_{30}t) - \exp(-k_1 t)] \tag{2b}$$

$$K^{(2)}(t) \approx 0 \tag{2c}$$

$$K^{(1)}(t) = K^{(1)}(0)\ \exp(-k_1 t) \tag{2d}$$

$$K^{(0)}(t) = K - K^{(1)}(t) - K^{(3)}(t) \tag{2e}$$

where $K^{(1)}(0)$ is the initial population in $|1\rangle$, K is the total concentration of absorbers and k_1 is the total decay rate for $|1\rangle$, which is equal to $k_{10}+k_{13}$. The rate constant k_{10} contains contributions from both a radiative rate k_{10}^{r} and a non-radiative rate k_{10}^{nr}, with $k_{10}=k_{10}^{r}+k_{10}^{nr}$.

Based on this model, an expression for $S_{54.7°}(t)$ can be readily obtained (see Appendix). In the small signal limit the magic angle signal is given by

$$S_{54.7°}(t) \approx K_1(0)d[\Delta\sigma^{(1)}K^{(1)}(t)+\Delta\sigma^{(3)}K^{(3)}(t)] \quad (3)$$

where

$$\Delta\sigma^{(1)}=\sigma_{01}-\sigma_{12} \quad (4a)$$

$$\Delta\sigma^{(3)}=\sigma_{01}-\sigma_{34} \quad (4b)$$

and d is the length of the pump–probe overlap region in the sample. In the absence of excited state absorption (i.e. $\sigma_{12}=\sigma_{34}=0$) the magic angle signal will be given by the sum of the populations for $|1\rangle$ and $|3\rangle$. This leads to bi-exponential decay kinetics for the magic angle signal:

$$S_{54.7°}(t) \approx \sigma_{01}K_1(0)d[(1-\Phi_3)\exp(-k_1t) + \Phi_3\exp(-k_{30}t)] \quad (5)$$

where $\Phi_3=k_{13}/k_1$, which is the yield of formation of state $|3\rangle$. In this expression we have assumed $k_1 \gg k_{30}$. Although bi-exponential kinetics are still obtained with excited state absorption, the pre-exponential coefficients depend on both the yield of formation of $|3\rangle$ and the differences in the absorption cross-sections. If the rate of the non-radiative transition from $|1\rangle$ to $|3\rangle$ is extremely fast compared with the rate of transition from $|1\rangle$ to $|0\rangle$ (i.e. $k_{10} \ll k_{13}$), the decay of the pump–probe signal will be dominated by the long-lived component. This is consistent with the absence of fluorescence from the complex. The fluorescence quantum yield is given by $\Phi_f=k_{10}^{r}/(k_{10}+k_{13})$. Low fluorescence yields occur for $k_{13} \gg k_{10}$ and k_{10}^{r}. Interestingly, others have noted that the broadness and lack of vibronic structure within the electronic absorption band of the complex are manifestations of a very short excited singlet state lifetime [17].

Because of the wavelength dependence of the absorption cross-sections, the proportion of components in the decay should vary with wavelength. This could explain why the pump–probe signal can be fitted by a single exponential decay function at 600 nm and a bi-exponential decay function at 570 nm. However, the short decay component obtained from the fit of the 570 nm data is much too long for there to be no fluorescence. Another explanation is that the amylose–iodine complex is heterogeneous and that there is a distribution of excited state lifetimes corresponding to different chromophores in different microenvironments. The bi-exponential decay observed for the amylose–iodine complex could therefore be due to the chromophore being located on different sites in the amylose helix. A more likely explanation is that at 570 nm other polyiodide chains are being excited. The shorter polyiodide chains absorb at shorter wavelengths. Indeed, monomeric I_5^- absorbs at about 559 nm [16] whereas $(I_5^-)_x$ absorbs at about 635 nm. Overlapping absorption bands will give rise to the multi-exponentially decaying signals in these single-wavelength pump–probe measurements. If our data were of higher quality, this non-exponentiality would probably also be evident for excitation at 600 nm. The 600 nm ground state recovery time of 870 ± 50 ps must therefore be considered as an average over a distribution of lifetimes. With better data we would also be able to carry out a lifetime distribution analysis to discern whether the two-component nature of the signal at 570 nm is due perhaps to two chromophores with very different lifetimes or is simply a pecularity of the shape of the distribution.

If an effective anisotropy $r^{(i)}(t,\boldsymbol{\mu}^{ij})$ is assigned to each optically allowed transition with cross-section σ_{ij}, then the observed anisotropy for the five-level model is given by (see Appendix)

$$r_{\text{observed}}(t)=\frac{\Delta r^{(1)}K^{(1)}(t)+\Delta r^{(3)}K^{(3)}(t)}{\Delta\sigma^{(1)}K^{(1)}(t)+\Delta\sigma^{(3)}K^{(3)}(t)} \quad (6)$$

where

$$\Delta r^{(1)}=\sigma_{01}r^{(0)}(t,\boldsymbol{\mu}^{01})-\sigma_{12}r^{(1)}(t,\boldsymbol{\mu}^{12}) \quad (7a)$$

$$\Delta r^{(3)}=\sigma_{01}r^{(0)}(t,\boldsymbol{\mu}^{01})-\sigma_{34}r^{(3)}(t,\boldsymbol{\mu}^{34}) \quad (7b)$$

Knowledge of the mechanisms for the loss of polarization would allow us to obtain explicit expressions for $r^{(i)}$. Even without knowing these mechanisms, information about the excited state dynamics can still be gleaned from the properties of the observed anisotropy in terms of the five-level model. First, an initial anisotropy which is less than the maximum value of 0.4 is consistent with the presence of excited state absorption. At zero time the population in $|3\rangle$ is zero (see Eq. (2b)). Consequently, the observed anisotropy at zero time will be determined by the anisotropy difference for ground state and excited state absorption from the first level of the singlet manifold, weighted by the corresponding absorption cross-sections:

$$r_{\text{observed}}(0)=\frac{\sigma_{01}r^{(0)}(0,\boldsymbol{\mu}^{01})-\sigma_{12}r^{(1)}(0,\boldsymbol{\mu}^{12})}{\sigma_{01}-\sigma_{12}} \quad (8)$$

In the absence of excited state absorption the anisotropy will be determined by the effective anisotropy for the $|0\rangle$-to-$|1\rangle$ optical transition with a value of 0.4. However, if excited state absorption is significant and the ground state dipole moment $\boldsymbol{\mu}^{01}$ is oriented differently from the excited state dipole moment $\boldsymbol{\mu}^{12}$, the observed anisotropy can be less than 0.4. Owing to the rapid decay of $K^{(1)}$, the observed anisotropy at longer times will be governed by the anisotropy difference between ground state and excited state absorption from the third level of the second manifold, weighted by the corresponding absorption cross-sections, i.e. for $t \gg 1/k_1$,

$$r_{\text{observed}}(t) \approx \frac{\Delta r^{(3)}}{\Delta\sigma^{(3)}} \quad (9)$$

The high value of the anisotropy, even after relaxation into level $|3\rangle$, is indicative of an ordered molecular system, as

expected for a linear polyiodide chain, with very little excitation energy transport. The absence of excitation-intensity-dependent decay kinetics is a signature that the excitation is not localized on a single I_5^- unit but is probably delocalized over a larger domain within the $(I_5^-)_x$ chain, in analogy to J-aggregate systems [13].

5. Conclusions

Despite the lack of fluorescence and the broadness of the absorption band of the amylose–iodine complex, a surprisingly long average relaxation time (about 870 ± 50 ps) is observed for the magic-angle-induced transmission at 600 nm, corresponding to excitation on the short wavelength side of the absorption band. This discrepancy can be resolved if one assumes that the photophysics of amylose–iodine is governed by two manifolds of levels: a manifold of singlet states and a manifold of "dark" states. In the context of the five-level model the absorption spectrum is due to a transition from the ground state to the first excited state of the singlet manifold. The lack of fluorescence is characteristic of fast non-radiative relaxation from the first singlet excited state, with the relaxation apparently being dominated by a non-radiative transition from this state to a low-lying state within the dark manifold. An anisotropy that is constant and equal to 0.35 ± 0.04 can be rationalized by excited state absorption within the singlet manifold. The constancy of the anisotropy is evidence for a highly ordered molecular system, as expected for a quasi-one-dimensional linear polyiodide chain, with the excitation delocalized over several I_5^- units. The clearly non-exponential character of the signal at 570 nm is probably more of a reflection of the microheterogeneity of the system and not due to any wavelength dependence in the level kinetics. Our future plans are to perform pump–probe experiments that will allow us to excite at one wavelength and probe with continuum light over a much longer time range (from nanoseconds to microseconds). By obtaining the transient spectra and studying their behavior in the presence of triplet quenchers and electron acceptors/donors, we will be able to determine the nature of the long-lived state in the amylose–iodine complex. Finally, we hope to extend these optical studies to other polymer–polyiodide systems.

Acknowledgements

E.L.Q. thanks the Robert A. Welch Foundation and the Texas Advanced Research Program for supporting this research.

Appendix

Following the approach of Alavi et al. [15], one can write expressions for the state populations for the five-level model for probe light polarized parallel and perpendicular to the pump light:

$$N_{\parallel}^{(2)}(t,\boldsymbol{\mu}^{2j}) \approx 0 \tag{A1a}$$

$$N_{\perp}^{(2)}(t,\boldsymbol{\mu}^{2j}) \approx 0 \tag{A1b}$$

$$N_{\parallel}^{(4)}(t,\boldsymbol{\mu}^{4j}) \approx 0 \tag{A1c}$$

$$N_{\perp}^{(4)}(t,\boldsymbol{\mu}^{4j}) \approx 0 \tag{A1d}$$

$$N_{\parallel}^{(3)}(t,\boldsymbol{\mu}^{3j}) = \tfrac{1}{3}K^{(3)}(t)[1+2r^{(3)}(t,\boldsymbol{\mu}^{3j})] \tag{A1e}$$

$$N_{\perp}^{(3)}(t,\boldsymbol{\mu}^{3j}) = \tfrac{1}{3}K^{(3)}(t)[1-r^{(3)}(t,\boldsymbol{\mu}^{3j})] \tag{A1f}$$

$$N_{\parallel}^{(1)}(t,\boldsymbol{\mu}^{1j}) = \tfrac{1}{3}K^{(1)}(t)[1+2r^{(1)}(t,\boldsymbol{\mu}^{1j})] \tag{A1g}$$

$$N_{\perp}^{(1)}(t,\boldsymbol{\mu}^{1j}) = \tfrac{1}{3}K^{(1)}(t)[1-r^{(1)}(t,\boldsymbol{\mu}^{1j})] \tag{A1h}$$

$$N_{\parallel}^{(0)}(t,\boldsymbol{\mu}^{0j}) = \tfrac{1}{3}K - \tfrac{1}{3}[K^{(1)}(t)+K^{(3)}(t)] \times [1+2r^{(0)}(t,\boldsymbol{\mu}^{0j})] \tag{A1i}$$

$$N_{\perp}^{(0)}(t,\boldsymbol{\mu}^{0j}) = \tfrac{1}{3}K - \tfrac{1}{3}[K^{(1)}(t)+K^{(3)}(t)] \times [1-r^{(0)}(t,\boldsymbol{\mu}^{0j})] \tag{A1j}$$

In these equations K is the total absorber concentration and $K^{(i)}(t)$ is the population in state $|i\rangle$ (see Eqs. (2a)–(2e)). For states $|0\rangle$, $|1\rangle$ and $|3\rangle$ the effective anisotropies are defined as

$$r^{(0)}(t,\boldsymbol{\mu}^{0j}) = \frac{N_{\parallel}^{(0)}(t,\boldsymbol{\mu}^{0j}) - N_{\perp}^{(0)}(t,\boldsymbol{\mu}^{0j})}{-[K^{(1)}(t)+K^{(3)}(t)]} \tag{A2a}$$

$$r^{(1)}(t,\boldsymbol{\mu}^{1j}) = \frac{N_{\parallel}^{(1)}(t,\boldsymbol{\mu}^{1j}) - N_{\perp}^{(1)}(t,\boldsymbol{\mu}^{1j})}{K^{(1)}(t)} \tag{A2b}$$

$$r^{(3)}(t,\boldsymbol{\mu}^{3j}) = \frac{N_{\parallel}^{(3)}(t,\boldsymbol{\mu}^{3j}) - N_{\perp}^{(3)}(t,\boldsymbol{\mu}^{3j})}{K^{(3)}(t)} \tag{A2c}$$

Equations (A2b) and (A2c) are standard definitions for excited state anisotropies. Eq. (A2a) for the ground state expression incorporates a modification that is necessary for the correct normalized value at $t=0$. In the small signal limit the Beer law transmission coefficients for the probe light after passage of the pump light are therefore given by

$$T_{\parallel}(t) = \exp\{-[\sigma_{01}N_{\parallel}^{(0)}(t,\boldsymbol{\mu}^{01}) + \sigma_{12}N_{\parallel}^{(1)}(t,\boldsymbol{\mu}^{12}) + \sigma_{34}N_{\parallel}^{(3)}(t,\boldsymbol{\mu}^{34})]d\} \tag{A3a}$$

$$T_{\perp}(t) = \exp\{-[\sigma_{01}N_{\perp}^{(0)}(t,\boldsymbol{\mu}^{01}) + \sigma_{12}N_{\perp}^{(1)}(t,\boldsymbol{\mu}^{12}) + \sigma_{34}N_{\perp}^{(3)}(t,\boldsymbol{\mu}^{34})]d\} \tag{A3b}$$

In these equations σ_{ij} is not the usual absorption cross-section but is a factor of 3 larger. The observed signals are related to these transmission coefficients by

$$S_{\parallel}(t) = \frac{T_{\parallel}(t) - T_{\parallel}(\infty)}{T_{\parallel}(\infty)} \tag{A4a}$$

$$S_{\perp}(t) = \frac{T_{\perp}(t) - T_{\perp}(\infty)}{T_{\perp}(\infty)} \tag{A4b}$$

Substitution of Eqs. (A1e)–(A1j) into Eqs. (A3a) and (A3b) yields in the small limit the following expressions for the signals:

$$S_{\parallel}(t) \approx \tfrac{1}{3}[\Delta\sigma^{(1)}K^{(1)}(t) + \Delta\sigma^{(3)}K^{(3)}(t)]d + \tfrac{2}{3}[\Delta r^{(1)}K^{(1)}(t) + \Delta r^{(3)}K^{(3)}(t)]d \quad \text{(A5a)}$$

$$S_{\perp}(t) \approx \tfrac{1}{3}[\Delta\sigma^{(1)}K^{(1)}(t) + \Delta\sigma^{(3)}K^{(3)}(t)]d - \tfrac{1}{3}[\Delta r^{(1)}K^{(1)}(t) + \Delta r^{(3)}K^{(3)}(t)]d \quad \text{(A5b)}$$

where $\Delta\sigma^{(1)}$ and $\Delta\sigma^{(3)}$ are given by Eqs. (4a) and (4b) and $\Delta r^{(1)}$ and $\Delta r^{(3)}$ are given by Eqs. (7a) and (7b). The magic angle signal is defined as

$$S_{54.7°}(t) = S_{\parallel}(t) + 2S_{\perp}(t) \quad \text{(A6)}$$

Substituting Eqs. (A5a) and (A5b) into Eq. (A6) results in Eq. (3). Finally, the observed anisotropy (Eq. (6)) can be obtained by substituting Eqs. (A5a) and (A5b) into Eq. (1).

References

[1] D.O. Cowan and F.M. Wiygul, *Chem. Eng. News,* (July 21, 1986) 28, and references cited therein.

[2] F. Cramer, U. Bergmann, P.C. Manor, M. Noltmeyer and W. Saenger, *Justus Liebigs Ann. Chem., 7–8* (1976) 1169.

[3] T.J. Marks, *Ann. NY Acad. Sci., 313* (1978) 594.

[4] L.C. Hardy and D.F. Shriver, *J. Am. Chem. Soc., 108* (1986) 2887.

[5] A. Philipp and C. Seeger, *Phys. Status Solidi, 689* (1978) 187.

[6] S.L. Hsu, A.J. Signorelli, G.P. Pez and R.H. Baughman, *J. Chem. Phys., 69* (1978) 106.

[7] D.A. Skoog, D.M. West and F.J. Holler, *Fundamentals of Analytical Chemistry,* Saunders, New York, 1992, p. 374.

[8] L. Stryer, *Biochemistry,* Freeman, New York, 1988, pp. 341–343.

[9] W. Banks and C.T. Greenwood, *Starch and its Components,* Aberdeen University Press, Edinburgh, 1975, pp. 67–112, and references cited therein.

[10] (a) R.E. Rundle and R. Baldwin, *J. Am. Chem. Soc., 65* (1943) 544; (b) R.E. Rundle and D. French, *J. Am. Chem. Soc., 65* (1943) 558; (c) R.E. Rundle and D. French, *J. Am. Chem. Soc., 65* (1943) 1707; (d) R.E. Rundle and F.C. Edwards, *J. Am. Chem. Soc., 65* (1943) 2200; (e) R.R. Baldwin, R.S. Bear and R.E. Rundle, *J. Am. Chem. Soc., 66* (1944) 111; (f) R.E. Rundle, J.F. Foster and R.R. Baldwin, *J. Am. Chem. Soc., 66* (1944) 2116; (g) R.E. Rundle, *J. Am. Chem. Soc., 69* (1947) 1769; (h) R.S. Stein and R.E. Rundle, *J. Chem. Phys., 16* (1947) 195.

[11] (a) J.M. Reddy, K. Knox and M.B. Robin, *J. Chem. Phys., 40* (1964) 1082; (b) M.B. Robin, *J. Chem. Phys., 40* (1964) 3369.

[12] (a) R.C. Teitelbaum, S.L. Ruby and T.J. Marks, *J. Am. Chem. Soc., 100* (1978) 3215; (b) R.C. Teitelbaum, S.L. Ruby and T.J. Marks, *J. Am. Chem. Soc., 102* (1980) 3322.

[13] (a) E.L. Quitevis, M.-L. Horng and S.-Y. Chen, *J. Phys. Chem., 92* (1988) 256; (b) S.-Y. Chen, M.-L. Horng and E.L. Quitevis, *J. Phys. Chem., 93* (1989) 3683; (c) M.-L. Horng and E.L. Quitevis, *J. Phys. Chem., 93* (1989) 6198; (d) E.L. Quitevis and M.-L. Horng, *Proc. SPIE, 1209* (1990) 198; (e) M.-L. Horng and E.L. Quitevis, *J. Phys. Chem., 97* (1993) 12 408.

[14] H. Isci and W.R. Mason, *Inorg. Chem., 24* (1985) 271.

[15] D.S. Alavi, R.S. Hartman and D.H. Waldeck, *J. Chem. Phys., 92* (1990) 4055.

[16] M. Mizuno, J. Tanaka and I. Harada, *J. Phys. Chem., 85* (1981) 1789.

[17] E. Mulazzi, I. Pollini, L. Piseri and R. Tubino, *Phys. Rev. B, 24* (1981) 3555.